Journal of Fluorine Chemistry 130 (2009) 749–754

Contents lists available at ScienceDirect

Journal of Fluorine Chemistry

journal homepage: www.elsevier.com/locate/fluor

Studies on fluoride adsorption capacities of amorphous Fe/Al mixed hydroxides from aqueous solutions

M.G. Sujana *, G. Soma, N. Vasumathi, S. Anand

Institute of Minerals and Materials Technology (Formerly RRL), Bhubaneswar 751 013, Orissa, India

ARTICLE INFO

Article history:
Received 5 March 2009
Received in revised form 28 May 2009
Accepted 6 June 2009
Available online 16 June 2009

Keywords:
Fluoride
Adsorption
Iron/aluminum mixed hydroxides
Kinetics and isotherm

ABSTRACT

This study evaluated the effectiveness of amorphous iron and aluminum mixed hydroxides in removing fluoride from aqueous solutions. A series of mixed Fe/Al samples were prepared at room temperature by co-precipitating Fe and Al mixed salt solutions at pH 7.5. The compositions (Fe:Al molar ratio) of the oxides were varied as 1:0, 3:1, 2:1, 1:1 and 0:1 and the samples were characterized by XRD, BET surface area and pH_{ZPC}. The XRD studies indicated the amorphous nature of the samples and Al(III) incorporation on Fe(III) hydroxides. Batch adsorption studies for fluoride removal on these materials showed that the adsorption capacities of the materials were highly influenced by solution pH, temperature and initial fluoride concentration. The rate of adsorption was fast and equilibrium was attained within 2 h. The adsorption followed first-order kinetics with intraparticle diffusion as the rate determining step for all the samples. The experimental data fitted well to both Langmuir and Freundlich adsorption isotherms. All samples exhibited very high Langmuir adsorption capacities; the sample with molar ratio 1 has shown maximum adsorption capacity of 91.7 mg/g. The thermodynamic parameters were determined to study the feasibility of the adsorption process.

1. Introduction

Fluoride is a persistent and non-degradable poison that accumulates in soil, plants, wild life and in humans. Fluoride can be enriched in natural waters by geological processes; there can also be formidable contributions from industries. High-fluoride containing wastewaters are generated by thermal power plants, rubber, fertilizer and semiconductor manufacturing, glass and ceramic production and electroplating industries. Severe chronic and cumulative over exposure can cause the incurable crippling of skeletal fluorosis. The problem is more acute in rural and small urban communities particularly in the third world countries [1,2]. The dental and skeletal fluorosis is irreversible and no treatment exists. The only remedy is prevention by keeping fluoride intake within the safe limits. The WHO has set a optimum fluoride level of 1.5 mg L^{-1} in drinking water for good health [3].

Various technologies such as adsorption, ion exchange, precipitation, electro-dialysis and reverse osmosis have been employed for fluoride removal from water [4–7]. Several conventional and non-conventional adsorbents were studied for their fluoride adsorption capacities [8–11]. Among these adsorbents, activated alumina is the most widely used because of its availability and inexpensiveness. However, it requires frequent regeneration because of its low adsorption capacity at neutral pH, which results in increased difficulty for operation and it also leads to increased dissolved aluminum in treated water [12].

In the recent years considerable attention has been devoted to develop cost effective novel adsorbent with high adsorption capacities. Iron and aluminum oxides are of great importance in industrial and technological applications due to their unique adsorptive properties for anions and cations and their occurrence as weathering products. These oxides are ubiquitous constituents of soils occurring both as discrete particles and as coatings on the surfaces of other soil constituents [13]. Amorphous iron and aluminum oxides demonstrate high specific surface areas and couples with the reactive nature of their surface functional groups, these components exhibit high capacity to retain heavy metal contaminants [14,15]. The charge on these hydroxyl surface functional groups is controlled by pH, at low pH, protonation will encourage the formation of positively charged $\equiv M{-}OH^{+}$ groups while at high pH deprotonation will promote negative $\equiv M{-}O^{-}$ groups. Although considerable work has been carried out on pure systems of aluminum and iron oxides for water treatment, very limited work has been reported on mixed oxyhydroxides of iron and aluminum for water treatment. The influence of the iron/aluminum molar ratio on heavy metal retention capacities, arsenate and arsenite removal capacities have been reported [16,17]. The iron based adsorbents prepared by sol–gel method

---

* Corresponding author. Tel.: +91 0674 2581639; fax: +91 0674 2581637.
E-mail address: mgsujana@gmail.com (M.G. Sujana).

0022-1139/$ – see front matter © 2009 Elsevier B.V. All rights reserved.
doi:10.1016/j.jfluchem.2009.06.005

have shown considerable enhancement of the adsorption capacities for fluoride [18,19]. The studies on crystalline mixed oxides of Fe/Al and Fe/Zr prepared at 65 and 80 °C on fluoride removal capacities were discussed and adsorption capacities of 17 and 8.2 mg g^{-1} respectively were reported [20–22]. So far, we have not come across the literature on amorphous iron and aluminum hydroxides with different molar ratios for fluoride removal. In the present study, an attempt was made to develop high surface area novel adsorbents based on Fe and Al content. The samples were prepared at room temperature by simple co-precipitation method and used for fluoride removal from aqueous solutions. This study provides an insight into the effect of varying molar ratio of Fe/Al on the physico-chemical properties and fluoride retention capacities.

2. Results and discussion

2.1. Characterization of materials

The XRD pattern of Fe:Al hydroxides is given in Fig. 1, the amorphous nature of the materials was conformed by X-ray diffraction patterns. Two broad peaks with *d*-values in the range of 2.54–2.57 and 1.47–1.48 corresponding to two line ferrihydrate (JCPDS No. 77.0247) were observed in all the samples except for pure aluminum hydroxide. The 3:1, 2:1and 1:1 samples have almost identical XRD patterns to that of pure ferrihydrate (1:0). No additional peaks corresponding to aluminum hydroxide were observed due to the amorphous nature of the Fe/Al samples. The pure Al sample showed four major XRD peaks for gibbsite phase with corresponding *d*-values of 4.82, 3.73, 2.99, 2.61, 2.34, 2.17, 2.04 and 1.93 Å (JCPDS No. 76-1782). The pH_{PZC} along with BET surface area values of all the samples are given in Table 1. All the samples have shown high specific surface area values, surface area increased with the decrease of molar ratio. The sample with molar ratio 1 has shown markedly high specific surface area of 268 $m^2\ g^{-1}$. Similar observations were reported by other researchers for co-precipitated Fe/Al oxides with molar ratio = 1, and were interpreted due to Al^{3+} species interference with the formation of large iron oxide particles and there by increasing the total surface area [15].

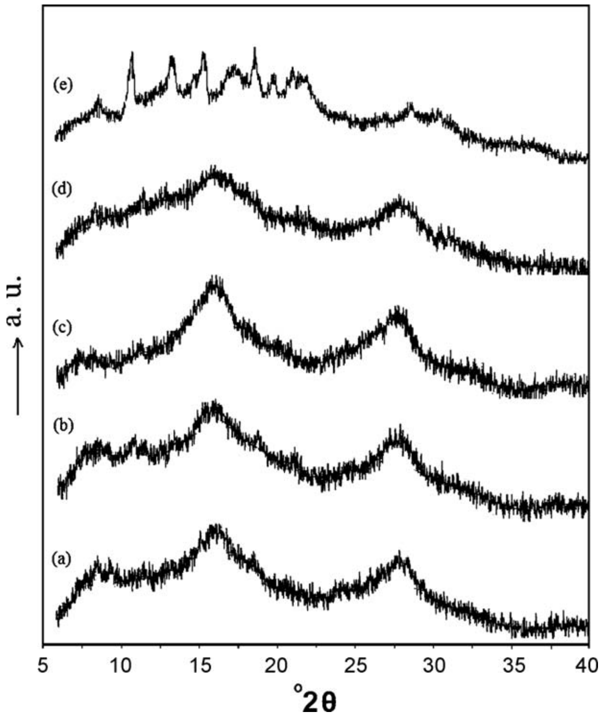

Fig. 1. XRD patterns of synthetic pure and mixed Fe/Al hydroxides (a) Fe, (b) 3 Fe:Al, (c) 2 Fe:Al, (d) Fe:Al and (e) Al.

Table 1
pH_{ZPC} and specific surface area values of the samples.

Adsorbent	Molar Fe/Al ratio	Zero point of charge (pH_{ZPC})	Specific surface area ($m^2\ g^{-1}$)
Fe:0	n.a.	4.8	231.6
3 Fe:Al	3	4.8	234.8
2 Fe:Al	2	5.1	245.6
Fe:Al	1	5.4	268.0
0:Al	n.a.	6.1	108.0

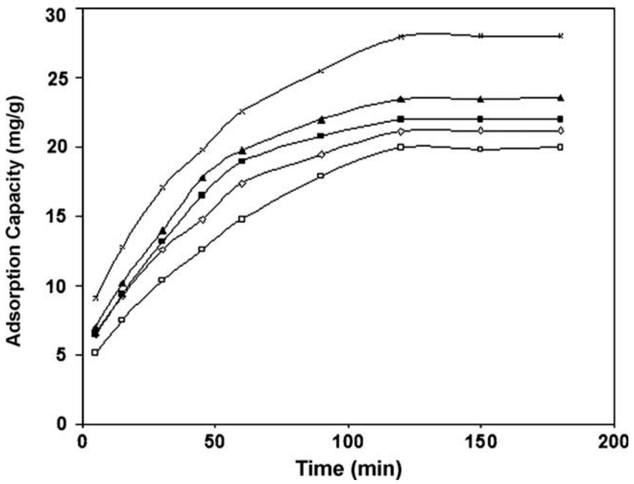

Fig. 2. Effect of contact time on fluoride removal studies (adsorbent dose 0.5 g L^{-1}, initial fluoride concentration 20 mg L^{-1}, temperature 30 °C and pH 4 for samples (◇) Fe, (■) 3 Fe:Al, (▲) 2 Fe:Al, (×) Fe:Al and (□) Al).

2.2. Effect of contact time

Fig. 2 shows the effect of contact time on fluoride sorption capacity by different synthetic samples. It reveals that with a fixed amount of adsorbent, the fluoride concentration in the solution decreased with contact time and for all the samples the equilibrium condition was around 2 h.

2.3. Sorption kinetics

The sorption rate constants of fluoride sorption on all five samples were determined to understand the adsorption phenomena in terms of the adherence of fluoride on the active sites of the adsorbent as well as its intraparticle diffusion within the pores of the adsorbent [26]. The time-dependent adsorption data have been analyzed by the following widely used kinetic equations.

A simple kinetics of sorption may be described by the pseudo-first-order equation which is in the form of [27]

$$\frac{dq_t}{dt} = k_1(q_e - q_t) \tag{1}$$

Integrating Eq. (1) and applying the boundary conditions $q_t = 0$ at $t = 0$ and $q_t = q_t$ at $t = t$, gives

$$\log(q_e - q) = \log\ q_e - \left(\frac{k_1}{2.303}\right)t \tag{2}$$

where, q_e and q_t are the amount of fluoride adsorbed at equilibrium and any time t (mg/g) respectively, and k_1 is the rate constant of pseudo-first-order sorption ($time^{-1}$). The plot of $\log(q_e - q)$ versus

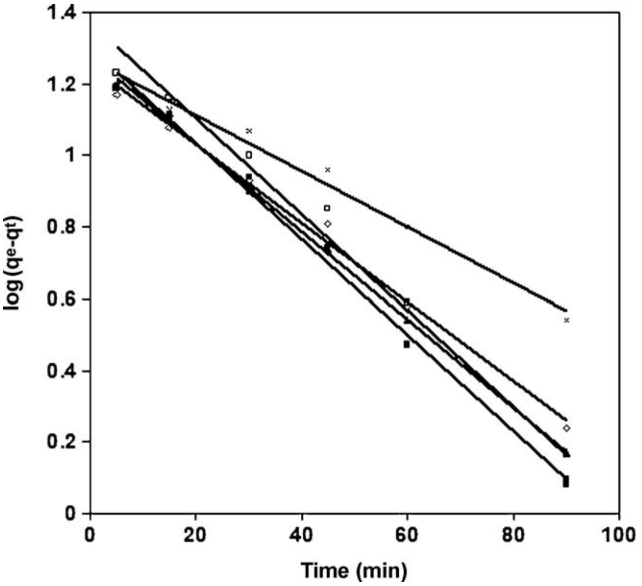

Fig. 3. Lagergren plots for the removal of fluoride (data corresponding to Fig. 2).

t (Fig. 3) at a fixed adsorbate, adsorbent dose, pH and temperature results in a straight line, which indicates applicability of Lagergren equation and first-order kinetics. The adsorption rate constant k_1 values were calculated from the slope of the plots and found to be 2.99, 3.84, 2.94, 1.79 and 3.17×10^{-1} $\text{min}^{-1}$for 1:0, 3:1, 2:1, 1:1 and 0:1 respectively.

Besides adsorption at the outer surface of the adsorbent, the fluoride ions may also diffuse into the interior of the porous adsorbent [28]. The intraparticle diffusion is the rate controlling factor; uptake of the adsorbate varies with the square root of the time. For the rate constant of intraparticle diffusion the equation can be written as,

$$q_t = q_i\sqrt{t} \tag{3}$$

where k_i is the intraparticle diffusion rate constant (mg/(g min$^{0.5}$)) and q_t is the amount of fluoride adsorbed at any time t (mg/g). Fig. 4 shows the intraparticle diffusion plots for different samples, the linearized form of the plots representing the control of adsorption by intraparticle diffusion. The k_i values of different samples were calculated from the slopes of the straight line portions of the respective plots and were found to be 1.77, 1.81, 1.67, 1.76 and 1.97 mg/(g min$^{0.5}$).

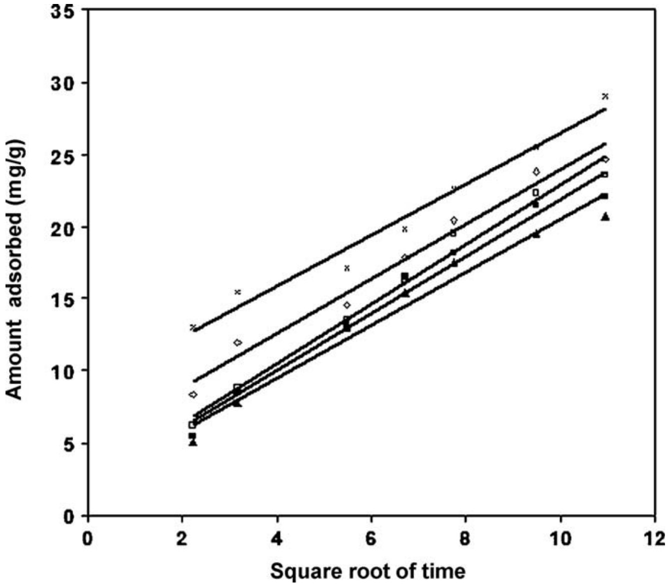

Fig. 4. Plots of amount of fluoride adsorbed versus square root of time for intraparticle diffusion (data corresponding to Fig. 2).

2.4. Effect of solution pH

Anions can be adsorbed on metal oxides through specific and/or nonspecific adsorption. The specific adsorption, involves ligand exchange reactions where the anions displace OH^- and/or H_2O from the surface [29]. The nonspecific adsorption involves the coulombic forces, and mainly depends on the pH_{pzc} of the sorbent [30]. The effect of solution pH on fluoride removal by different synthetic materials was studied in the range of 2.5–10 and the results are shown in Fig. 5. In all the cases, sorption passes through maxima. Therefore, the pH-dependent interaction of fluoride on hydrous metal oxides can be represented schematically as follows:

$$\equiv MOH + H^+ \leftrightarrow \equiv MOH_2^+ \tag{4}$$

$$\equiv MOH_2^+ + F^- \leftrightarrow \equiv MF + H_2O \tag{5}$$

which in combination gives

$$\equiv MOH + H^+ + F^- \leftrightarrow \equiv MF + H_2O \tag{6}$$

This two step mechanism is favorable at acidic pH, at pH >6 fluoride ions are predominantly adsorbed by following mechanism

$$\equiv MOH + F^- \leftrightarrow \equiv MF + HO^- \tag{7}$$

where M represents metal ion (Fe or Al), MOH represents a surface hydroxyl group and MF a surface site occupied by a fluoride ion. Eqs. (4)–(6) represent the electrostatic interaction between positively charged metal oxide surface and negatively charged fluoride ions in the acidic pH range. The fluoride adsorption capacity on metal oxide surface becomes pronounced in this pH range. Eq. (7) represents the ligand exchange interactions between the fluoride ion and hydroxyl groups that found to occur at the neutral pH region. For the samples 1:0, 3:1 and 2:1 optimum pH range for fluoride removal was found to be around

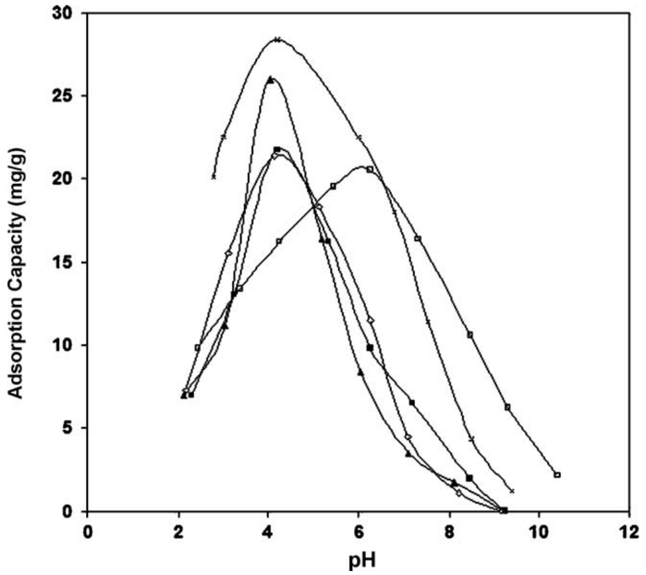

Fig. 5. Effect of solution pH on fluoride removal by hydrous mixed and pure oxides (adsorbent dose 0.5 g L^{-1}, initial fluoride concentration 20 mg L^{-1}, temperature 30 °C and contact time 2 h for samples (◇) Fe, (■) 3 Fe:Al, (▲) 2 Fe:Al, (×) Fe:Al and (□) Al).

4–5, whereas, for samples 1:1 and 0:1 wide optimum pH range for fluoride removal was found (4–7.5), this may be due to both specific and nonspecific adsorption on these surfaces. Further decrease of adsorption in the alkaline pH may be due to the competition of the hydroxyl ions with the fluoride for surface sites or electrostatic repulsion of fluoride ion to the negatively charged surface.

2.5. Isotherm study

The experimental data obtained for different initial fluoride concentrations at constant temperature and pH was taken for isotherm study. The two adsorption isotherms, namely the Langmuir or Freundlich isotherms models were used to analyze the adsorption data. The Langmuir and Freundlich isotherm equations applied for the study are given below:

$$\frac{C_e}{q_e} = \frac{1}{Q_o b} + \frac{C_e}{Q_o} \tag{8}$$

$$\log\ q_e = \log\ K_F + \frac{1}{n}\log\ C_e \tag{9}$$

where C_e is equilibrium concentration (mg/L), q_e is the amount adsorbed at equilibrium (mg/g), Q_o is adsorption capacity for Langmuir isotherms and 'b' is an energy term which varies as a function of surface coverage strictly due to variations in the heat of adsorption. The constant, 'n' indicates the degree of favorability of adsorption [31] and K_F is the isotherm constant for Freundlich model. Initial fluoride concentrations of fluoride from 10 to 100 mg L^{-1} were studied, Fig. 6 shows the adsorption isotherm plots of equilibrium concentration versus fluoride adsorbed per unit mass of adsorbent. The adsorption data of fluoride on all the samples was fitted to both Langmuir and Freundlich isotherm models as shown in Figs. 7 and 8. The calculated isotherm parameters along with correlation coefficients are given in Table 2. The magnitude of the Langmuir constant 'b' has small values (0.033–0.061 L/mg), which indicates a low heat of adsorption. The "n" value increased with the increase of Al content in the samples, which indicates the increase of bond strength between adsorbate and adsorbent and it also indicates the adsorbent surface to be of heterogeneous [32,33]. The Langmuir adsorption capacities of our samples are much higher than the reported values for fluoride in the literature (Table 3).

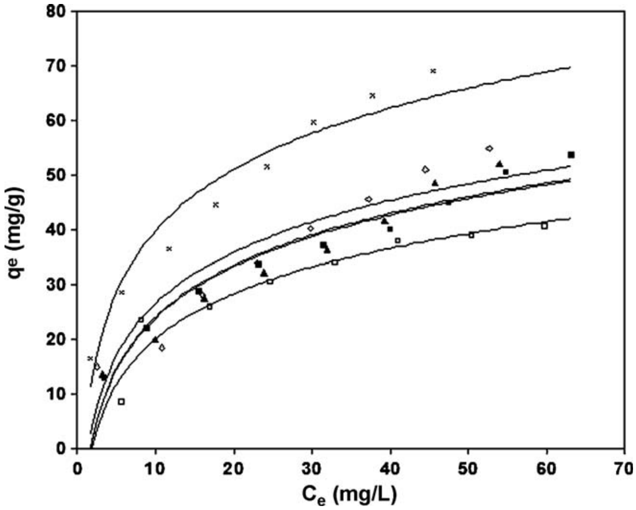

Fig. 6. Adsorption isotherms of hydrous mixed and pure oxides for different initial fluoride concentrations (adsorbent dose 0.5 g L^{-1}, pH 4, contact time 2 h and temperature 30 °C for samples (◇) Fe, (■) 3 Fe:Al, (▲) 2 Fe:Al, (×) Fe:Al and (□) Al).

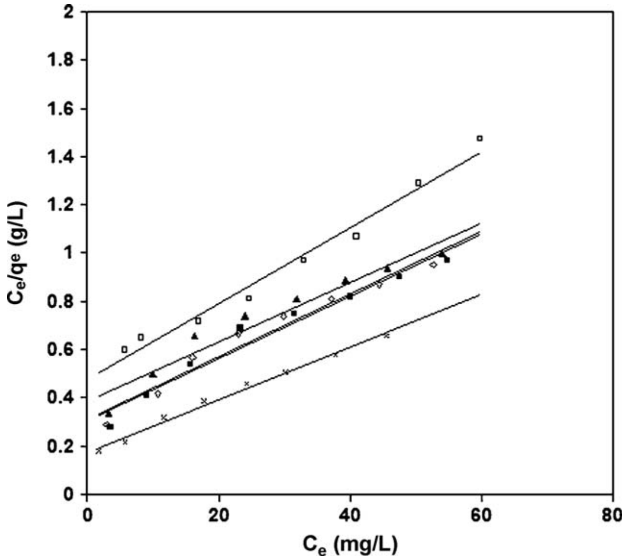

Fig. 7. Langmuir plots for adsorption of fluoride.

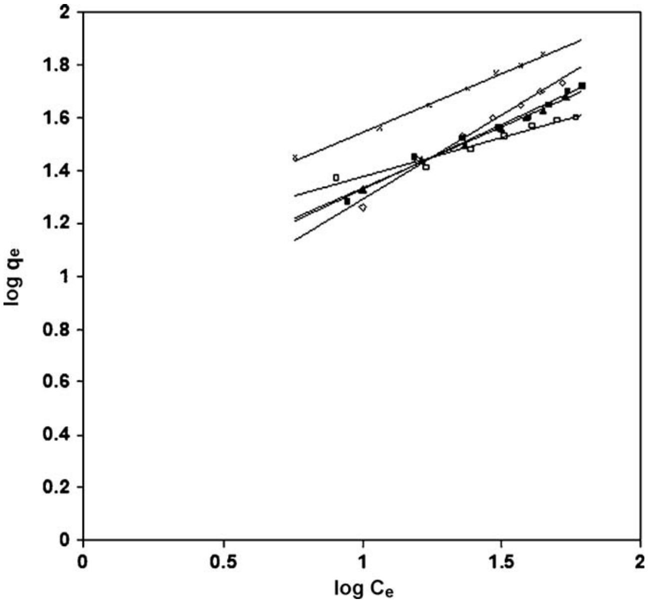

Fig. 8. Freundlich plots for fluoride adsorption.

Table 2
Calculated isotherm parameters for Langmuir and Freundlich models.

S. No.	Langmuir isotherm			Freundlich isotherm		
	R^2	Q_o (mg g^{-1})	b	R^2	K_F	n
Fe	0.95	76.9	0.041	0.98	4.36	1.56
3 Fe:Al	0.95	78.1	0.041	0.98	6.76	2.04
2 Fe:Al	0.94	81.3	0.031	0.98	7.24	2.17
Fe:Al	0.99	91.7	0.061	0.99	12.59	2.27
Al	0.98	63.5	0.033	0.95	11.74	3.45

2.6. Effect of temperature

As adsorption process is associated with several thermodynamic parameters, the temperature dependence was studied in the range of 30–60 °C. The solution pH (4.1), concentrations of adsorbate (20 mg L^{-1}) and adsorbent (0.5 g L^{-1}) were kept constant and equilibrations were made for 2 h. For the samples 1:0, 3:1, 2:1 and 1:1 adsorption capacity increased with the

Table 3
Fluoride adsorption capacities of different sample.

S. No	Adsorbent	Langmuir adsorption capacity (mg g^{-1})	Reference
1.	Crystalline Fe/Al oxides	17.7	[21]
2.	Aluminum type super para-magnetic adsorbent	38	[9]
3.	Magnetic chitosan particle	20–23	[10]
4.	Hydrous ferric oxide	16.5	[35]
5.	Fe:Al hydrous oxide	91.7	Present work
6.	$Fe(OH)_3$	76.98	Present work

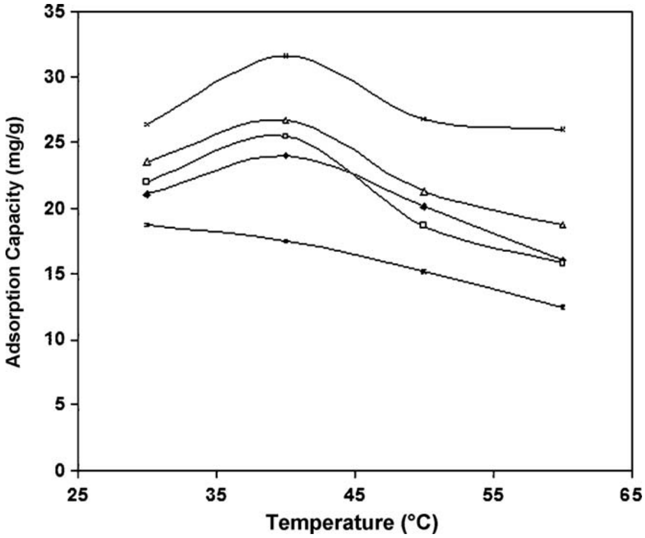

Fig. 9. Effect of temperature on fluoride removal (initial fluoride concentration 20 mg L^{-1}, adsorbent dose 0.5 g L^{-1}, pH 4 and contact time 2 h for samples (◇) Fe, (■) 3 Fe:Al, (▲) 2 Fe:Al, (×) Fe:Al and (□) Al).

increase in temperature from 30 to 40 °C and increase in temperature from 40 to 60 °C showed decreasing trend (Fig. 9). Chemisorption and physisorption employed simultaneously in these samples. Other researchers have reported that the fluoride adsorption on crystalline Fe/Al mixed oxide increased with rise in temperature from 10 to 40 °C [21]. Fluoride adsorption capacity of pure aluminum hydroxide (0:1) decreased with the increase in temperature, showing the exothermic nature of adsorption. In order to study the feasibility of the process, the thermodynamic parameters were obtained from the following equations

$$K_C = \frac{C_{Ae}}{C_e} \tag{10}$$

$$\Delta G^o = -RT\ln\ K_C \tag{11}$$

$$\log\ K_C = \frac{\Delta S^o}{2.303R} - \frac{\Delta H^o}{2.303TR} \tag{12}$$

where C_e is the equilibrium concentration in solution in mg/L and C_{Ae} is the equilibrium concentration on the adsorbent in mg/L and K_C is the equilibrium constant. The van't Hoff plots (not shown) of ln K_C against $1/T$ were used to find out thermodynamic parameters. The thermodynamic parameters obtained were given in Table 4. The negative ΔG^o values indicate that the adsorption of fluoride on all the samples is favorable and spontaneous under standard conditions. The negative ΔH^o values confirm the adsorption to be exothermic in nature for all the samples. Generally, adsorption processes are associated with positive values of ΔS^o, though negative values of ΔS^o for adsorption on some heterogeneous materials have also been reported [34].

Table 4
Thermodynamic parameters for the fluoride removal on pure and mixed Fe/Al hydroxides.

Sample	ΔG^o (kJ/mol)	ΔS^o (J/(K mol))	ΔH^o (kJ/mol)
Fe	−0.27	−80.24	−25.34
3 Fe:Al	−0.50	−96.07	−29.98
2 Fe:Al	−0.90	−54.94	−17.793
Fe:Al	−1.67	−62.80	−21.98
Al	−0.10	−61.39	−18.45

3. Conclusions

In this study, amorphous Fe/Al based novel adsorbents with high specific surface areas were developed by simple co-precipitation method at room temperature. The increase of Al content in $Fe(OH)_3$ matrix slightly increased the surface area and pH_{ZPC} values. The fluoride adsorption on these materials is encouraging, the equilibrium time data for all samples followed first-order kinetics and was governed by intraparticle diffusion model. The optimum pH range for fluoride adsorption was found to be 4–5 for the samples 1:0, 3:1 and 2:1, whereas it is in the range of 4–7.5 for 1:1 and 0:1.The equilibrium data fitted to both Langmuir and Freundlich isotherm models and showed high adsorption capacities. The thermodynamic studies demonstrate that the fluoride adsorption on these materials is thermodynamically favorable, spontaneous and exothermic in nature.

4. Experimental

4.1. Synthesis of adsorbents and their characterization

Chemicals used in this work were procured from MERCK, India Ltd. The stock solutions of $Al(NO_3)_3$ and $Fe(NO_3)_3$ were used to prepare series of samples at different initial Fe:Al molar ratios. Five combinations of amorphous oxides, which include pure iron and aluminum hydroxides with Fe:Al ratio of 1:0, 3:1, 2:1, 1:1 and 0:1 were prepared by adding required 1 M KOH to a continuously stirred solution of iron and aluminum with a total strength of 0.1 moles. The product pH was raised to 7.5 (±0.1) and stirring was continued for 1 h and the suspension was then filtered and washed repeatedly with warm double distilled water. The precipitates were then dried at 60 °C in hot air oven, powdered and stored in an air tight container for further use. The concentrations of iron and aluminum in the samples were determined by digesting the sample in 5N HCl and analyzing with a Perkin Elmer Atomic Absorption Spectrophotometer. The amorphous nature and mineral phase compositions were determined by X-ray diffraction (XRD) measurements which were done over a range of 5°–40° using Phillips Powder Diffractometer (Model PW3710) with Mo K_α radiation at a scan speed of 1.2°/min. All the pH measurements were carried out by Consort digital pH meter (231). The pH_{pzc} of prepared samples were determined by solid addition method [23]. The detailed procedure is described in our earlier publication [24]. Fluoride analysis was carried out by following SPADNS method [25] and the color absorbance was measured at 570 nm on Thermo Water analysis Spectrophotometer (Model AquaMate). The specific surface areas of samples were determined using Quantasorb, Quantachrome Corporation, USA.

4.2. Adsorption experiments

Batch experiments were performed for determination of equilibrium time and kinetics and to identify the isotherm. A 100 mg L^{-1} fluoride stock solution was prepared by dissolving 0.221 g of sodium fluoride in 1 L of double distilled water at room temperature. The experimental solutions were prepared by appropriate dilutions of the above solution. Adsorption studies were carried out at different conditions *viz.* contact time (05–180 min), pH (2.5–10), initial fluoride concentrations (10–90 mg L^{-1}) and temperature (305–333 K). About 25 mg of the sample was taken in a 100 mL polyethylene plastic vial and 50 mL of fluoride solution of known concentration was added. The contents (adsorbent/water 0.5 g L^{-1}) were kept for constant shaking in a temperature controlled water bath shaker for required time and then the solids were separated by centrifuging at 3500 rpm on REMI centrifuge. The solutions were collected for analysis and fluoride concentration in the solutions was determined. Each experiment was conducted three times and average values are reported. The sorption capacity X (mg g^{-1}) of the adsorbent was calculated from the following equation

$$X = \left(\frac{C_i - C_e}{C_A}\right)$$

where C_e is the residual concentration reached at equilibrium state, C_i is the initial fluoride concentration and C_A is the adsorbent concentration.

Acknowledgements

The authors are thankful to Prof. B.K. Mishra, Director, Institute of Minerals and Materials Technology (IIMT), Bhubaneswar, for his kind permission to publish this work.

References

[1] K. Kim, G.Y. Jeong, Chemosphere 58 (2005) 1339–1408.
[2] G. Kartikeyan, A. Shunmugasundaraj, Fluoride 33 (2000) 121–127.
[3] WHO, Chemical fact sheets: fluoride. In guidelines for drinking water quality (electronic resource): incorporation first addendum, Recommendations vol. 1, 3rd ed., Geneva, pp. 375–377, 2006.
[4] M. Young, T. Hashimoto, N. Hosho, H. Myoga, Water Res. 33 (1999) 3395–3402.
[5] A.M. Raichur, M.J. Basu, Sep. Purif. Technol. 24 (2001) 121–127.
[6] Y.H. Li, S. Wang, A. Cao, D. Zhao, X. Zhang, C. Xu, Z. Luan, J. Liang, D. Ruan, D. Wu, B. Wei, Chem. Phys. Lett. 350 (2001) 412–416.
[7] Y. Wang, E.J. Reardon, Appl. Geochem. 16 (2001) 531–539.
[8] C.-F. Chang, P.-H. Lin, W. Holl, Colloids Surf. A: Physicochem. Eng. Aspects 280 (2006) 194–202.
[9] W. Ma, F.-Q. ya, M. Han, R. Wang, J. Hazard. Mater. 143 (2006) 296–302.
[10] M.G. Sujana, R.S. Thakur, S.B. Rao, J. Colloid Interface Sci. 275 (1998) 355–359.
[11] H. Farrah, J. Slavek, W.F. Pickering, Aust. J. Soil Res. 25 (2008) 55–69.
[12] P.P. Coetzee, L.L. Coetzee, R. Puka, S. Mubenga, Water SA 29 (2003) 331–338.
[13] A. Violante, M. Pigna, Soil Sci. Soc. Am. J. 66 (2002) 1788–1796.
[14] R.M. Cornell, U. Schwertmann, The Iron Oxides: Structure, Properties, Reactions, Occurrence and Uses, VCH, Weinheim, Germany, 1996, p. 573.
[15] P.R. Anderson, M.M. Benjamin, Environ. Sci. Technol. 24b (1990) 1586–1592.
[16] X. Meng, R.D. Letterman, Environ. Sci. Technol. 27 (1993) 1924–1929.
[17] H.A.B. Potter, R.N. Yong, Appl. Clay Sci. 14 (1999) 1–26.
[18] A. Violante, M. Ricciardella, M. Pigna, Water Air Soil Pollut. 145 (2003) 289–306.
[19] N.I. Chubar, V.F. Samanidou, V.S. Kouts, G.G. Gallios, V.A. Kanibolotsky, V.V. Strelko, I.Z. Zhuravlev, J. Colloid Interface Sci. 291 (2005) 67–74.
[20] X. Wu, Y. Zhang, X. Dou, M. Yang, Chemosphere 69 (2007) 1758–1764.
[21] K. Biswas, S.K. Saha, U.C. Ghosh, Ind. Eng. Chem. Res. 46 (2007) 5346–5356.
[22] K. Biswas, D. Bandhoyapadhyay, U.C. Ghosh, Adsorption 13 (2007) 83–94.
[23] L.S. Balistreiri, T.T. Chao, Soil Sci. Soc. Am. J. 51 (1987) 1145–1151.
[24] M.G. Sujana, H.K. Pradhan, S. Anand, J. Hazard. Mater. 161 (2008) 120–125.
[25] A.E. Greenberg, L.S. Coesreri, A.D. Eaton (Eds.), Standard Methods For the Examination of Water and Waste Water, John Wiley & Sons, New York, 1987, p. 325.
[26] R. Leyva-Ramos, J.R. Rangel-Mendez, L.A. Bernal-Jacome, M.S. Berber-Mendoza, J. Chem. Technol. Biotechnol. 580 (2005) 924–933.
[27] S. Lagergren, Zur theorie der sogenannten adsorption gelöster stoffe, Kungliga Svenska Vetenskapsakademiens, Handlingar 24 (4) (1898) 1–39.
[28] M. Mahramanlioglu, I. Kizilcikli, I.O. Bicer, J. Fluorine Chem. 115 (2002) 41–47.
[29] D.M. Ruthven, Principles of Sorption and Sorption Processes, John Wiley & Sons, New York, 1984 (Chapter 6).
[30] P.D. Rude, R.C. Aller, Am. J. Sci. 293 (1993) 1–24.
[31] E.R. Treybal, Mass Transfer Operations, Chemical Engineering Series, 3rd ed., McGraw Hill International editions, Singapore, 1981.
[32] M. Doğan, J. Hazard. Mater. 109 (2004) 141–148.
[33] K.K. Pandey, G. Prasad, V.N. Singh, J. Chem. Technol. Biotechnol. 34A (1984) 367–374.
[34] M. Sarkar, A. Banerjee, P.P. Pramanick, A.R. Sarkar, J. Colloid Interface Sci. 302 (2006) 432–441.
[35] S. Dey, S. Goswami, U.C. Ghosh, Water Air Soil Pollut. 158 (2004) 311–323.